Water Science & Technology

IWA PUBLISHING

Optimization of the electrochemical oxidation of textile wastewater by graphite electrodes by response surface methodology and artificial neural network

Mohammed Saleh[a], Rabia Yildirim[a], Zelal Isik[a], Ahmet Karagunduz[b], Bulent Keskinler[b] and Nadir Dizge[a,*]

[a] Department of Environmental Engineering, Mersin University, Mersin, 33343, Turkey
[b] Department of Environmental Engineering, Gebze Technical University, Kocaeli, 41400, Turkey
*Corresponding author. E-mail: ndizge@mersin.edu.tr

ABSTRACT

In this study, electrochemical oxidation of combed fabric dyeing wastewater was investigated using graphite electrodes. The response surface methodology (RSM) was used to design the experiments via the central composite design (CCD). The planned experiments were done to track color changes and chemical oxygen demand (COD) removal. The experimental results were used to develop optimization models using RSM and the artificial neural network (ANN) and they were compared. The developed models by the two methods were in good agreement with the experimental results. The optimum conditions were found at 150 A/m^2, pH 5, and 120 min. The removal efficiencies for color and COD reached 96.6% and 77.69%, respectively. The operating cost at the optimum conditions was also estimated. The energy and the cost of 1 m^3 of wastewater required 34.9 kWh and 2.58 US$, respectively. The graphite electrodes can be successfully utilized for treatment of combed fabric dyeing wastewater with reasonable cost.

Key words: artificial neural network, combed fabric dyeing wastewater, response surface method, electro oxidation, graphite electrodes

HIGHLIGHTS

- Electrochemical oxidation of combed fabric dyeing wastewater was investigated using graphite electrodes.
- The optimum conditions were found at 150 A/m^2, pH 5, and 120 min.
- The removal efficiencies for the color and COD reached 96.60% and 77.69%, respectively.

INTRODUCTION

The textile industry is a competitive industry that has a crucial role in any developed/developing community. Unfortunately, the textile industries produce a large amount of wastewater (GilPavas et al. 2020). According to Neill et al. (1999), a large amount of water (125–250) L is required for 1 kg of the finished product (Neill et al. 1999). Thus the textile industry produces enormous wastewater quantities with dyestuff, surfactants, and additives, which have dangerous effects on the environment and humans (Aravind et al. 2016; Saleh et al. 2019a).

In the last decade, several methods were examined to treat textile wastewater. Yagub and colleagues (2014) reviewed the use of adsorption in dye removal from the aqueous solutions (Yagub et al. 2014). The regeneration of the adsorbent and the production of secondary pollutants have limited the process (Yalvaç et al. 2020). Membrane technology was also applied to treat and recycle textile wastewater (Cengiz Yatmaz et al. 2017; Nadeem et al. 2019). The initial cost and the fouling issues had not favored the membrane filtration (Lin et al. 2016). Coagulation and flocculation methods were also employed (Verma et al. 2012), but the possibility of generating extra sludge had become a significant concern (Amaral-Silva et al. 2016). According to Soares et al. (2017), biological treatment may not be sufficient if applied alone (Soares et al. 2017). Advanced oxidation processes (AOPs) were implemented (Carvalho & Carvalho 2017). Despite their high performance, AOPs may generate other pollutants (Gągol et al. 2018). In regard to this, the electrochemical techniques have become more favorable because of their functionality, simplicity, safety, eco-friendliness, and low costs (Brillas & Martínez-Huitle 2015). The electrochemical treatment can degrade the pollutants in the textile wastewater via direct or indirect oxidation (Radjenovic & Sedlak 2015). The electrochemical techniques mainly include electrocoagulation/electro floatation, electro oxidation (EO), and electro reduction (Brillas & Martínez-Huitle 2015).

EO has become the most popular electrochemical technique because it eliminates the redox chemicals, facilitates the reaction control by managing the current or potential, and increases the onsite treatment possibility (Panizza & Cerisola 2005). The material of the anode can influence the electrochemical mechanism and the produced material (Särkkä et al. 2015). Lead and lead oxide (Awad & Abo Galwa 2005), boron-doped diamond (Koparal et al. 2007; Zhu et al. 2018; Kuchtová et al. 2020), dimensionally stable anode (DSA) (Tavares et al. 2012; Zhang et al. 2012), and activated carbon cloth (ACC) (Cukierman 2013) electrodes were used as a base for the electrode in the EO process. Graphite electrodes had the attention of the researchers because of their low cost, low resistivity, chemical inertness and good conductivity (Kariyajjanavar et al. 2013a, 2013b). The degradation of the dyes by graphite electrodes can occur via direct or indirect oxidation (Hamza et al. 2011). The direct oxidation occurs at the graphite surface or electron transfer directly to the graphite anode. The presence of chlorine in the textile wastewater effluents makes indirect oxidation the dominant degradation mechanism. The oxidation of chlorine at the graphite anode yields active species that can oxidize the pollutants (Isik et al. 2020).

The combed fabric dyeing wastewater has a high chlorine concentration (14,515 mg/L). Thus, the graphite electrode can be considered an attractive solution. This study aims to explore the removal efficiency of color and chemical oxygen demand (COD) from the combed fabric dyeing wastewater by graphite electrodes. The affecting parameters (pH, time, and applied current) were optimized. The traditional methods of optimization are not able to describe the complicated interaction among the variables and the responses (Taherkhani et al. 2018). The response surface methodology (RSM) is a mix of statistical and mathematical techniques that could be used to solve this issue (Körbahti & Demirbüken 2017; Gadekar & Ahammed 2019). The RSM starts with experiment design, followed by model fitting and verification, and ends with determining the optimum conditions step (Darvishmotevalli et al. 2019). In this study, the central composite design (CCD) was used to design the experiments. Furthermore, the artificial neural network (ANN) was used to model and optimize the electrooxidation process. ANN is another modeling technique that has the advantage of the ability to create a nonlinear relationship between the affecting factors and the proposed responses without any prior knowledge of the nature of the relationship (Elfghi 2016; Yabalak & Yilmaz 2019). The design matrix and the final pH values obtained from RSM were utilized to build an ANN neural network. In this way, the modeling results had a more precise prediction. So, the results from the two methods were compared and examined statistically. Finally, the operational cost of the EO of the combed fabric dyeing wastewater by the graphite electrodes at the optimum conditions was analyzed.

MATERIALS AND METHODS

Materials

Combed fabric dyeing wastewater was collected from a textile factory in Gaziantep province, Turkey. The wastewater was characterized based on the American Public Health Association Standard Methods (Rice et al. 2017). The characteristics are shown in Table 1.

Table 1 | Combed fabric dyeing wastewater characteristics

Parameter	Unit	Value
COD	mg/L	833
TSS	mg/L	12
Sulfate (SO$_4$)	mg/L	164
Total nitrogen	mg/L	51.3
Total Kjeldahl nitrogen	mg/L	47.8
pH	–	6.9
Conductivity	μS/cm	3,030
Color	Pt-Co	2,213
Chloride	mg/L	1,451

TSS. total suspended solids.
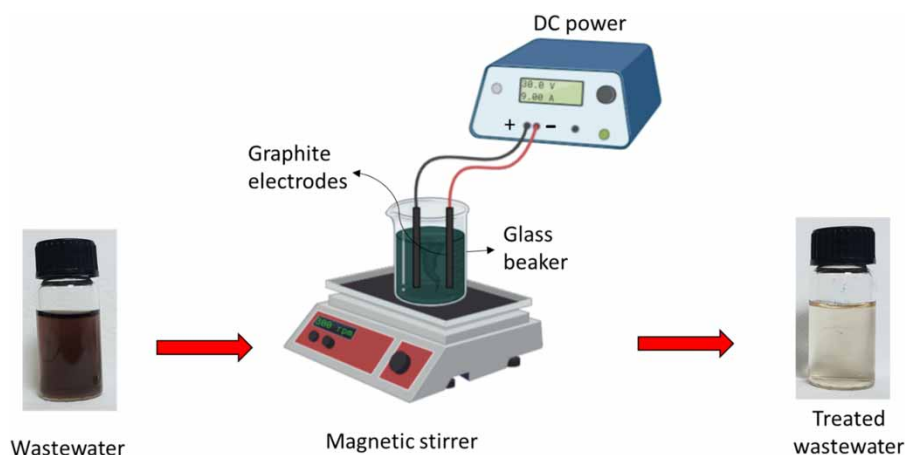
Experimental setup

The EO experiments were conducted in a batch reactor (Figure 1). The reactor consists of a 400 mL borosilicate glass reactor, two graphite electrodes with 5 cm width $\times$ 8 cm height $\times$ 2 mm thickness, a digital DC power supply (AATech ADC-3303D, Germany, maximum voltage of 30 V) with two connecting wires, and a magnetic stirrer (Wisd -Wisestir MSH-20A, Germany) with a Teflon-covered magnetic stirring bar. A sample of 200 mL of the textile wastewater was inserted inside the borosilicate glass reactor, followed by placing the electrode pairs with a 2 cm distance between them and connected to the DC power supply with the wires. The stirring process at 300 rpm continued simultaneously with the EO experiments.

At certain times, the samples were collected and centrifuged at 6,000 rpm for 5 min. The pH and the conductivity were measured by pH/Cond. 340i Handheld multi meter, WTW. Color changes were noticed by UV-visible spectrophotometer (Hach DR 3900) using Platinum–Cobalt (Pt-Co) method following the Standard Method No. 2120 (Rice *et al.* 2017). The chemical oxygen demand (COD) was measured using the closed reflux method-titrimetric method following Standard Method No. 5220C (Rice *et al.* 2017). The concentration of chloride before and after the EO process was measured by argentometric method following Standard Method No. 4500B (Rice *et al.* 2017). The removal efficiency was calculated using Equation (1).

$$Removal\ (\%) = \frac{Initial\ Concentration - Final\ Concentration}{Initial\ Concentration} \tag{1}$$

RSM and ANN

CCD as an approach in response surface methodology (RSM) was used to optimize the affecting parameter. CCD is a statistical method for multivariate nonlinear model development. The developed model can be used to explore the relationship between the parameters. CCD is also applied for regression model equations calculation. The applied current, pH, and time were used as model variables to design the experiments by Design Expert Version 11.0 [Stat-Ease]. The removal efficiencies obtained from the preliminary studies, α-values for the low and maximum level, and the economic perspectives were the basis for the ranges of the variables selection process. The ranges of the factors were selected based on many criteria. Table 2 represents the variables and their ranges. In total, 20 experiments were carried out to track the effects of the parameter changes on COD and color.

Figure 1 | Experimental setup for the electrooxidation.

Table 2 | Independent variables ranges

Variable	Unit	Factor	Low	High	$-\alpha$	$+\alpha$
Current	A/m^2	A	50	150	15.91	184.09
pH	–	B	5	9	3.64	10.36
Time	Min	C	60	120	39.55	140.45

ANN modeling was integrated with the RSM using the pH values at the end of the experiments. In the ANN, the network type was a feed-forward artificial neural network. The network included an input layer, a hidden layer, and an output layer. The experiment matrix in the CCD was used as a base for the ANN modeling. The input for the ANN was the experiment conditions in addition to the final pH. The output layer was the removal efficiencies for color and COD. The neurons required in the hidden layer were determined by trial and error to obtain the maximum regression with minimum errors. In this study four neurons were used. The designed ANN is shown in Figure 2.

RESULTS AND DISCUSSION

Color removal

CCD was used to study the effect of the independent variables on color removal. The results were tested by linear, two-factor interaction (2FI), quadratic, and cubic models. Based on their regression coefficients, the linear model was selected to represent the results. Table 3 shows the regression coefficients for the tested models.

The prediction ability of the developed model was also examined by the analysis of variance (ANOVA). According to Table 4, the model has a large F-value (101.97) and a p-value smaller than 0.0001. These values show that the model is significant and can be used in color removal prediction. The model was also found to be non-significant in the lack of fit test. The model has a predicted R^2 of 0.91 that reasonably agreed with the adjusted R^2 of 0.94 since the difference is less than 0.20. Also, the model has an adequate precision, since the model ratio 31.42 is larger than 4.

The removal of color can be expected using Equation (2).

$$Color\ Removal\ (\%) = 74.99 + 0.07 * Current - 0.17 * pH + 0.09 * Time \tag{2}$$

COD removal

COD removal by the EO method was also examined and modeled by the CCD method. The experimental results were fitted to the linear, 2FI, quadratic, and cubic models. The quadratic model had the highest regression values (Table 5). The quadratic

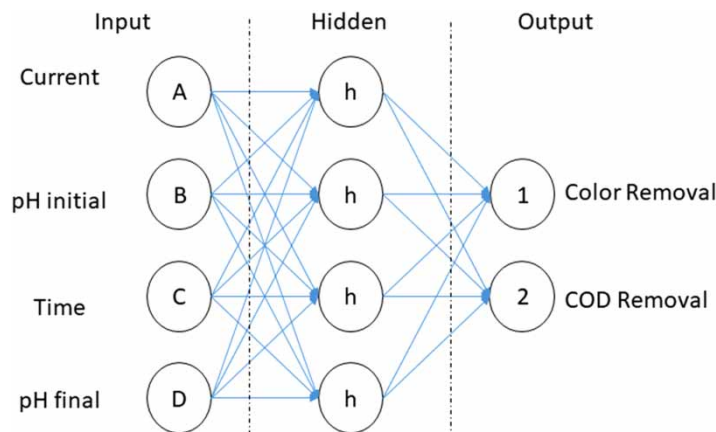**Figure 2** | The designed ANN.

Table 3 | Regression coefficients for the tested models

Source	Sequential p-value	Lack of fit p-value	Adjusted R^2	Predicted R^2	Note
Linear	1.22E-10	0.11	0.94	0.91	Suggested
2FI	0.18	0.13	0.95	0.87	–
Quadratic	0.50	0.10	0.95	0.82	–
Cubic	0.62	0.02	0.94	−1.77	Aliased

Table 4 | ANOVA and the lack of fit tests results for color removal

Source	Sum of squares	df	Mean	F-value	p-value
Model	250.11	3.00	83.37	101.97	1.22E-10
A-Current	146.76	1.00	146.76	179.50	4.10E-10
B-pH	1.63	1.00	1.63	1.99	0.18
C-Time	101.72	1.00	101.72	124.42	5.88E-09
Residual	13.08	16.00	0.82	–	–
Lack of Fit	11.45	11.00	1.04	3.19	0.10
Pure Error	1.63	5.00	0.33	–	–

Table 5 | Regression coefficients for the tested models for COD removal

Source	Sequential p-Value	Lack of fit p-value	Adjusted R^2	Predicted R^2	Note
Linear	0.16×10^{-3}	0.20×10^{-3}	0.65	0.50	–
2FI	0.96	0.11×10^{-3}	0.58	0.46	–
Quadratic	5.53×10^{-7}	0.07	0.97	0.91	Suggested
Cubic	0.50	0.02	0.97	−0.23	Aliased

Reduced Quadratic model : Adjusted R^2 0.97, Predicted R^2 0.95.

model was reduced to improve the regression factor and to have a better data description. The reduced quadratic model had an adjusted R^2 of 0.97, while the predicted R^2 was 0.95. The reduced quadratic model had adequate precision with a ratio of 44.12.

ANOVA was also applied for COD removal model. The model was found to be significant with F-value and p-value of 138.01 and <0.0001, respectively. The model was also examined by lack of fit test. According to the F-value (4.62), the model was a good fit, and the lack of fit is not significant. The significances of model terms were investigated and are shown in Table 6.

Accordingly, the developed model can be used to predict the removal efficiency of COD, as shown in Equation (3).

$$COD\ Removal\ (\%) = -3.482 + 1.068 * Current - 1.823 * pH + 0.115 * Time - 0.004\ Current^2 \tag{3}$$

ANN results

The ANN used to predict color and COD removal is shown in Figure 2. The developed ANN was tested by Leverberg Marquartz (LM) algorithm with log sigmoidal as a transform function (Hammoudi *et al.* 2019). Table 7 shows the performance of the network and the errors calculation based on different indicators.

Table 6 | ANOVA and the lack of fit tests results for COD removal

Source	Sum of squares	df	Mean square	F-value	p-value
Model	4,857.24	4.00	1,214.31	138.01	1.22×10^{-11}
A-Current	3,181.33	1.00	3,181.33	361.56	6.55×10^{-12}
B-pH	181.63	1.00	181.63	20.64	0.39×10^{-3}
C-Time	161.60	1.00	161.60	18.37	0.65×10^{-3}
A^2	1,332.68	1.00	1,332.68	151.46	3.06×10^{-9}
Residual	131.98	15.00	8.80	–	–
Lack of Fit	119.10	10.00	11.91	4.62	0.05
Pure Error	12.89	5.00	2.58	–	–

Table 7 | Performance indicator for color and COD removal models

| Performance	Color Removal		COD removal	
	RSM	ANN	RSM	ANN
MSE	0.65	0.15	6.6	1.24
RMSE	0.81	0.39	2.56	1.11
MAPE	0.73	0.26	4.71	0.93
R^2 predicted	0.91	0.98	0.95	0.97

The mean squared error (MSE) and root mean squared error (RMSE) for the ANN models (color and COD) were lower than the RSM models. The lower value means higher description and prediction capabilities (Gadekar & Ahammed 2019). Mean absolute percentage error (MAPE) test is a method to determine the accuracy of the model (Mohamed 2019). Lower values for the MAPE are favorable and mean the model is more accurate. In this case, the ANN models have lower values. ANN models have higher regression coefficients (R^2) (Saleh *et al.* 2019b). To ensure that the models are validated in describing the EO process, the experiments are conducted before and after the modeling process. The experimental results and the modeled results are shown in Table 8.

Parameters' effects

The effects of current density, pH, and time on the EO of combed fabric dyeing wastewater were explored. Combed fabric dyeing wastewater was exposed to varied current densities (50–150 A/m²). The current density is linearly proportional to color removal (Figure 3(a) and 3(b)). The maximum color removal (95%) occurred at the current 150 A/m², while the

Table 8 | The design matrix among the experimental results and the expected data

| Run	Current (A/m²)	pH	Time (min)	Color Removal (%)			COD removal (%)		
				Experimental	RSM	ANN	Experimental	RSM	ANN
1	100.00	10.36	90.00	88.61	87.94	88.80	52.89	56.58	52.88
2	15.91	7.00	90.00	81.92	83.01	82.48	8.26	10.10	8.31
3	100.00	7.00	90.00	88.34	88.52	88.37	59.80	62.72	62.64
4	100.00	7.00	90.00	88.40	88.52	88.37	62.81	62.72	62.64
5	50.00	5.00	120.00	88.39	88.32	88.14	43.18	45.01	43.18
6	100.00	7.00	90.00	88.32	88.52	88.37	62.81	62.72	62.64
7	150.00	9.00	60.00	89.38	88.73	89.37	62.00	61.36	61.37
8	50.00	5.00	60.00	82.83	82.86	82.44	44.63	38.13	48.41
9	150.00	5.00	120.00	96.60	94.88	96.59	77.69	75.54	77.69
10	150.00	5.00	60.00	90.06	89.42	89.68	67.98	68.66	67.98
11	100.00	7.00	39.55	82.91	83.93	82.80	58.68	56.93	58.66
12	184.09	7.00	90.00	92.91	94.04	92.80	59.71	61.43	59.71
13	100.00	7.00	90.00	88.36	88.52	88.37	64.81	62.72	63.45
14	100.00	3.64	90.00	88.79	89.11	89.29	63.84	68.85	63.81
15	50.00	9.00	60.00	82.83	82.17	82.55	28.72	30.84	28.85
16	50.00	9.00	120.00	88.48	87.63	88.33	40.29	37.72	40.27
17	100.00	7.00	90.00	88.34	88.52	88.37	62.81	62.72	62.64
18	100.00	7.00	140.45	92.50	93.11	92.51	69.42	68.50	69.38
19	150.00	9.00	120.00	92.77	94.19	92.76	71.07	68.24	71.07
20	100.00	7.00	90.00	89.75	88.52	88.37	62.81	62.72	62.64
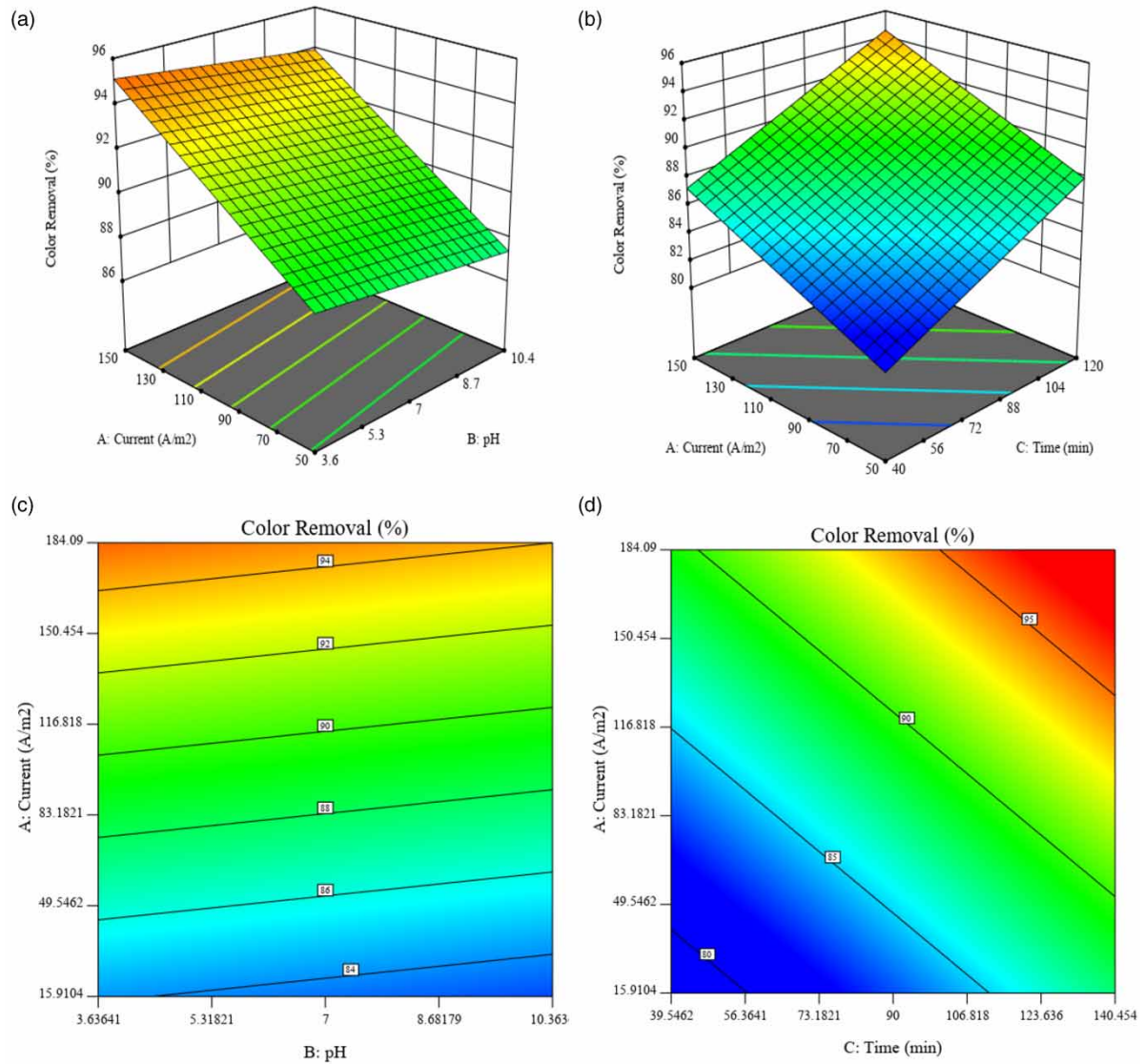
Figure 3 | (a) Surface color removal response for current and pH effects, (b) surface color removal response for current and time, (c) contour response for current and pH effects on color removal, (d) contour response for current and time effects on color removal.

minimum color removal was 82% at the current density of 50 A/m². Figure 3(c) and 3(d) show the contour map for the removal of color using the EO process with the changes in the current, pH, and time.

The removal efficiency of COD also increased with the current density (Figure 4(a)). The relationship between COD degradation and the applied current was found to be quadratic (Figure 4(b)). The maximum COD degradation at higher current density was 76%, while the minimum was 31% at a lower value (Figure 4(c)). As shown in Table 1, the textile wastewater contains chloride at a concentration of 1,451 mg/L. The chloride concentration decreased to 70 mg/L at the end of the reaction. In the EO method, chloride (Cl⁻) can be converted to different forms (Periyasamy & Muthuchamy 2018). Equation (4) presents the generation of chlorine (Cl₂) at the anode side, while Equation (5) shows the reaction at the cathode side (Rajkumar & Muthukumar 2017).

$$2Cl^- \rightarrow Cl_2 + 2e^- \tag{4}$$

$$2H_2O + 2e^- \rightarrow H_2 + 2OH^- \tag{5}$$
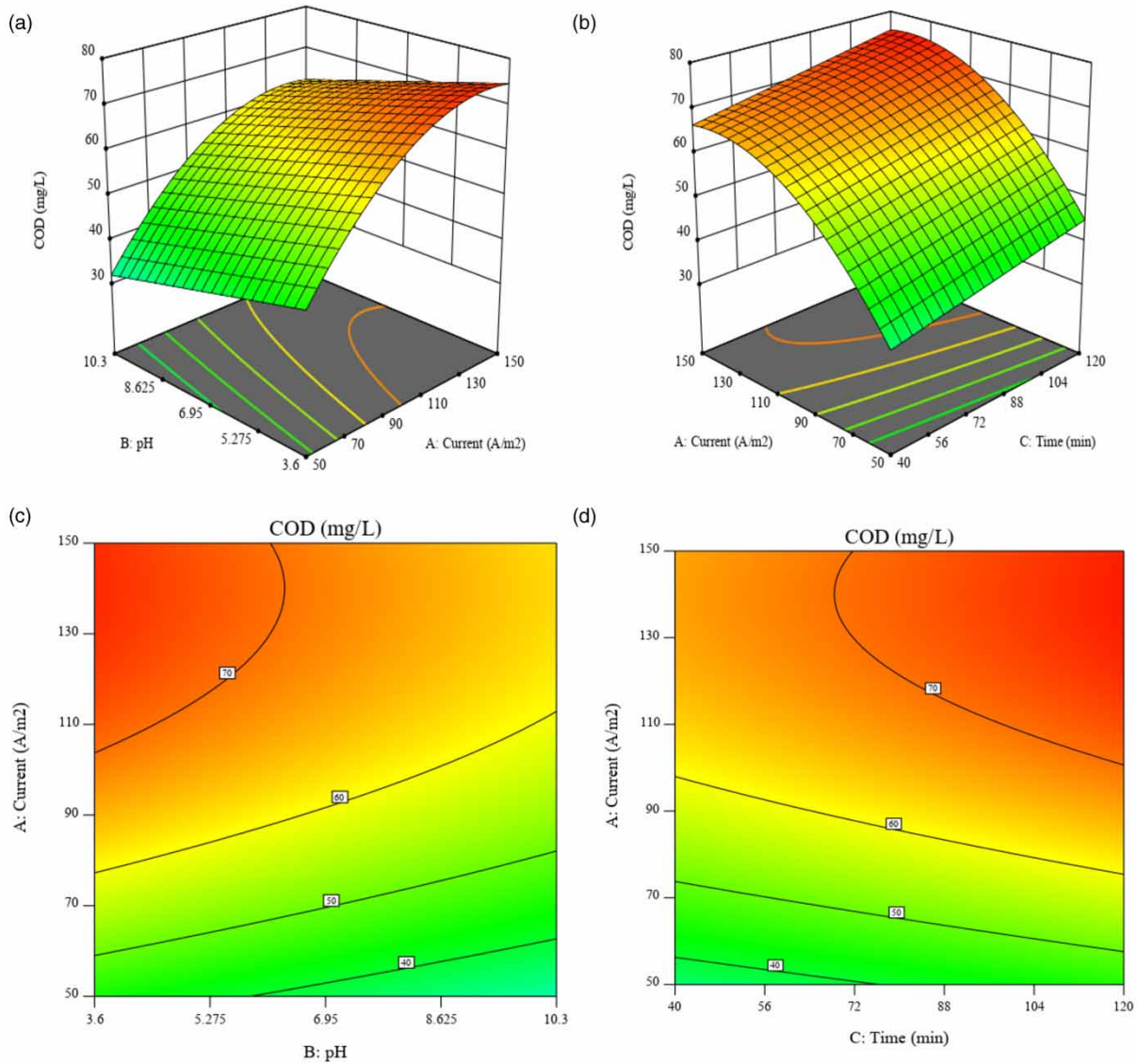
Figure 4 | (a) Surface COD removal response for current and pH effects, (b) surface COD removal response for current and time, (c) contour response for current and pH effects on COD removal, (d) Contour response for current and time effects on color removal.

The generated chlorine reacts with water to form hypochlorous acid (Equation (6)) (Sirés *et al.* 2014). Hypochlorous acid is a weak acid, which dissociates into hypochlorite and hydrogen ion, as shown in Equation (7) (Isik *et al.* 2020).

$$Cl_2 + H_2O \rightarrow HOCl + H^+ + Cl^- \tag{6}$$

$$HOCl \rightarrow H^+ + OCl^- \tag{7}$$

The increases in the removal of both color (Figure 3(c)) and COD (Figure 4(b)) with the increases in the current density can be related to the generation rate of hypochlorite. At higher current density, the generation rate of hypochlorite increases; consequently, the degradation of color and COD is also raised, as shown in Equation (8).

$$OCl^- + Pollutant \rightarrow Product + CO_2 + H_2O + Cl^- \tag{8}$$

The effect of pH was also optimized. Different experiments were conducted at different pH values (5–9). The removal efficiencies of color and COD had inverse relationships with pH (Figures 3(c) and 4(c)). The maximum removals for color and COD were found to be at pH 5, while the lowest values were at pH 9. In alkaline medium, the ionization of chlorine/hypochlorite ions is low (Isik et al. 2020). In addition to that, the production of chlorate or perchlorate is more favorable (Equation (9)). In the acidic medium, the generation of chlorine/chloride from the hypochlorous acid is higher (Equation (6)). The presence of chloride/chlorine in the wastewater increases the degradation efficiency, since it can oxidize the organic at the anode or in the solution (Mussa et al. 2015). Thus, the oxidation of COD and color at lower pH values (pH 5) is higher.

$$6OCl^- + 3H_2O \rightarrow \frac{3}{2}O_2 + 6H^+ + 2ClO_3^- + 4Cl^- + 6e^- \tag{9}$$

The optimum time required to degrade color and COD was found to be 120 min (Figures 3(d) and 4(d)). The removal efficiencies increased with the increase in time. At 60 min, the removal efficiencies for color and COD were 89 and 68%, respectively. The removal efficiencies increased to reach 95% for color and 76% for COD at 90 min.

The optimum conditions for textile wastewater treatment by graphite electrode were determined. The maximum color and COD removal were when the applied current reached 150 A/cm^2, pH was 5, and the reaction continued to 120 min. At the optimum conditions, color was removed with a percentage of 96.6% and COD was degraded with a percentage of 77.7%. The EO of textile wastewater by the graphite electrodes had successfully reduced color and COD to meet the Turkish discharge standards for textile industry wastewaters (Hukuk ve Mevzuat Genel Müdürlüğü 2004). Table 9 shows the initial and final concentrations along with the standard concentration.

Anode efficiency and cost analysis

The operation cost is the key factor in treating wastewater. In this study, a cost analysis was accomplished to determine the feasibility of using EO treatment of the textile wastewater by graphite electrode. The efficiency of the graphite electrode based on the specific energy was determined using Equations (10)–(12) (Dizge et al. 2018; Ukundimana et al. 2018).

$$\text{SEG (kWh/m}^3) = \frac{V_O \times I \times t}{1{,}000 \times V} \tag{10}$$

$$\text{SEG (kWh/kg color)} = \frac{V_O \times I \times t}{1{,}000 \times V \times (Color_i - Color_f)} \tag{11}$$

$$\text{SEG (kWh/kg COD)} = \frac{V_O \times I \times t}{1{,}000 \times V \times (COD_i - COD_f)} \tag{12}$$

where: SEG is the graphite electrode specific energy, V_O, I, t, and V are the applied voltage (V), current (A), time (h), and wastewater volume (m^3), respectively, and COD_i and COD_f are the initial and final chemical oxygen demand (kg/L).

The treatment cost for 1 m^3 of the textile wastewater was estimated by multiplying the SEG (kWh/m^3) by the cost of the kilowatts per hour. According to the Turkish Electricity Distribution Company, the cost of 1kwh is about 0.074 US$. Table 10 presents the cost analysis of the treatment of textile wastewater by EO at the optimum conditions.

The results in Table 9 show that the treatment of the textile wastewater by the EO method with a graphite electrode is efficient. The energy and the cost of 1 m^3 of wastewater required just 34.90 kWh and 2.58 US$, respectively. These results are lower than in the study by Isik and colleagues (2020), who used activated carbon cloth as electrodes (Isik et al. 2020). A comparison with other works is shown in Table 11.

Table 9 | Initial, final, and the standard values for the different parameters

	Unit	Initial value	Final value	Standard
Color	Pt-Co	2,213	75.2	260
pH	–	6.9	6.5	6–9
COD	mg/L	833	185.8	200

Table 10 | Cost analysis for the electro oxidation treatment of textile wastewater by graphite electrodes at the optimum conditions

Indicator	Unit	Value
SEG	kWh/m^3	34.90
SEG-Color	kWh/kg color	16.33
SEG-COD	kWh/kg COD	53.92
Energy cost	US\$/m^3	2.58

Table 11 | Comparison with other studies

Electrodes	Optimum conditions	Removal efficiency (%)	Energy consumption	Reference
Anode: Graphite Cathode: Graphite	Current density: 150 A/m^2 pH:5 Time: 120 min	COD: 77.69% Color: 96.6%	34.90 kWh/m^3	This study
Anode: ACC Cathode: ACC	Current density: 100 A/m^2 pH: 7 Time: 60 min	COD: 95.5% Color: 95.5%	36 kWh/m^3	Isik et al. (2020)
Anode: Expanded graphite/ attapulgite composite materials Cathode: Copper	Current density: 7.5 mA/cm^2 pH: 7 Time: 60 min	COD: 43.6% Color: 100%	–	Kong et al. (2009)
Anode: Ti/RuO$_2$ Cathode: Aluminum	Current density: 1.41 mA/cm^2 pH: 5.41 Time: 130 min	Color: 88%	–	Kaur et al. (2020)
Anode: BDD Cathode: Fe	Current density: 10 mA/cm^2 pH: 5.41 Time: 60 min	COD: 88% Color: 100%	3.83 USD/m^3	GilPavas et al. (2020)

BDD: boron-doped diamond.

CONCLUSION

The textile industry is a competitive industry that has a crucial role in any developed/developing community. Unfortunately, the textile industries produce a large amount of wastewater. The textile wastewater has large quantities of dyestuff, which have dangerous effects on the environment and humans. In this study, the treatment of combed fabric dyeing wastewater by graphite electrode was explored for the removal of color and COD. The affecting parameters (pH, time, and current) were optimized using RSM and ANN. As expected, the developed ANN has described the results more precisely. Based on the two models, the optimum conditions were found to be 150 A/m^2, pH 5, and 120 min. The removal efficiencies for color and COD reached 96.6% and 77.69%, respectively. The operating cost at the optimum conditions was also estimated. The energy and the cost of 1 m^3 of wastewater required just 34.90 kWh and 2.58 US\$, respectively. Although an efficient treatment application was utilized successfully to treat combed fabric dyeing wastewater, the graphite electrodes still suffer from carbon corrosion problems, which affects the EO process performance.

ACKNOWLEDGEMENT

DATA AVAILABILITY STATEMENT

All relevant data are included in the paper or its Supplementary Information.

REFERENCES

Amaral-Silva, N., Martins, R., Paiva, C., Castro-Silva, S. & Quinta-Ferreira, R. 2016 A new winery wastewater treatment approach during vintage periods integrating ferric coagulation Fenton reaction and activated sludge. *Journal of Environmental Chemical Engineering* **4**, 2207–2215.

Aravind, P., Subramanyan, V., Ferro, S. & Gopalakrishnan, R. 2016 Eco-friendly and facile integrated biological-cum-photo assisted electrooxidation process for degradation of textile wastewater. *Water Research* **93**, 230–241.

Awad, H. & Abo Galwa, N. 2005 Electrochemical degradation of Acid Blue and Basic Brown dyes on Pb/PbO$_2$ electrode in the presence of different conductive electrolyte and effect of various operating factors. *Chemosphere* **61**, 1327–1335.

Brillas, E. & Martínez-Huitle, C. 2015 Decontamination of wastewaters containing synthetic organic dyes by electrochemical methods. An updated review. *Applied Catalysis B: Environmental* **166–167**, 603–643.

Carvalho, S. & Carvalho, N. 2017 Dye degradation by green heterogeneous Fenton catalysts prepared in presence of *Camellia sinensis*. *Journal of Environmental Management* **187**, 82–88.

Cengiz Yatmaz, H., Dizge, N. & Kurt, M. S. 2017 Combination of photocatalytic and membrane distillation hybrid processes for reactive dyes treatment. *Environmental Technology* **38** (21), 2743–2751.

Cukierman, A. 2013 Development and environmental applications of activated carbon cloths. *ISRN Chemical Engineering* **2013**, 1–31.

Darvishmotevalli, M., Zarei, A., Moradnia, M., Noorisepehr, M. & Mohammadi, H. 2019 Optimization of saline wastewater treatment using electrochemical oxidation process: prediction by RSM method. *MethodsX* **6**, 1101–1113.

Dizge, N., Akarsu, C., Ozay, Y., Gulsen, H. & Adiguzel, S. 2018 Sono-assisted electrocoagulation and crossflow membrane processes for brewery wastewater treatment. *Journal of Water Process Engineering* **21**, 52–60.

Elfghi, F. 2016 A hybrid statistical approach for modeling and optimization of RON: a comparative study and combined application of response surface methodology (RSM) and artificial neural network (ANN) based on design of experiment (DOE). *Chemical Engineering Research and Design* **113**, 264–272.

Gadekar, M. R. & Ahammed, M. M. 2019 Modelling dye removal by adsorption onto water treatment residuals using combined response surface methodology-artificial neural network approach. *Journal of Environmental Management* **231**, 241–248.

Gągol, M., Przyjazny, A. & Boczkaj, G. 2018 Wastewater treatment by means of advanced oxidation processes based on cavitation–a review. *Chemical Engineering Journal* **338**, 599–627.

GilPavas, E., Dobrosz-Gómez, I. & Gómez-García, M.-Á. 2020 Efficient treatment for textile wastewater through sequential electrocoagulation, electrochemical oxidation and adsorption processes: optimization and toxicity assessment. *Journal of Electroanalytical Chemistry* **878**, 114578.

Hammoudi, A., Moussaceb, K., Belebchouche, C. & Dahmoune, F. 2019 Comparison of artificial neural network (ANN) and response surface methodology (RSM) prediction in compressive strength of recycled concrete aggregates. *Construction and Building Materials* **209**, 425–436.

Hamza, M., Ammar, S. & Abdelhedi, R. 2011 Electrochemical oxidation of 1,3,5-trimethoxybenzene in aqueous solutions at gold oxide and lead dioxide electrodes. *Electrochimica Acta* **56**, 3785–3789.

Hukuk ve Mevzuat Genel Müdürlüğü. 2004 *SU KİRLİLİĞİ KONTROLÜ YÖNETMELİĞİ*. Resmi Gazete, Ankara.

Isik, Z., Unal, B. O., Karagunduz, A., Keskinler, B. & Dizge, N. 2020 Electrochemical treatment of textile dye bath wastewater using activated carbon cloth electrodes. *Avicenna Journal of Environmental Health Engineering* **7** (1), 47–52.

Kariyajjanavar, P., Narayana, J. & Nayaka, Y. 2013a Electrochemical degradation of C.I. Vat brown 1 dye on carbon electrode. *Advanced Chemistry Letters* **1**, 32–39.

Kariyajjanavar, P., Narayana, J. & Nayaka, Y. A. 2013b Degradation of textile dye C.I. Vat black 27 by electrochemical method by using carbon electrodes. *Journal of Environmental Chemical Engineering* **1** (4), 975–980.

Kaur, P., Imteaz, M. A., Sillanpaa, M., Sangal, V. K. & Kushwaha, J. P. 2020 Parametric optimization and MCR-ALS kinetic modeling of electro oxidation process for the treatment of textile wastewater. *Chemometrics and Intelligent Laboratory Systems* **203**, 104027.

Kong, Y., Yuan, J., Wang, Z., Yao, S. & Chen, Z. 2009 Application of expanded graphite/attapulgite composite materials as electrode for treatment of textile wastewater. *Applied Clay Science* **46**, 358–362.

Koparal, A. S., Yavuz, Y., Gurel, C. & Ogutveren, U. B. 2007 Electrochemical degradation and toxicity reduction of C.I. Basic Red 29 solution and textile wastewater by using diamond anode. *Journal of Hazardous Materials* **145**, 100–108.

Körbahti, B. K. & Demirbüken, P. 2017 Electrochemical oxidation of resorcinol in aqueous medium using boron-doped diamond anode: reaction kinetics and process optimization with response surface methodology. *Frontiers in Chemistry* **5**, 75.

Kuchtová, G., Chýlková, J., Váňa, J., Vojs, M. & Dušek, L. 2020 Electro-oxidative decolorization and treatment of model wastewater containing acid blue 80 on boron doped diamond and platinum anodes. *Journal of Electroanalytical Chemistry* **863**, 114036.

Lin, J., Ye, W., Baltaru, M.-C., Tang, Y. P., Bernstein, N. J., Gao, P., Balta, S., Vlad, M., Volodin, A., Sotto, A., Luis, P., Zydney, A. L. & Bruggen, B. V. d. 2016 Tight ultrafiltration membranes for enhanced separation of dyes and Na$_2$SO$_4$ during textile wastewater treatment. *Journal of Membrane Science* **514**, 217–228.

Mohamed, Z. E. 2019 Using the artificial neural networks for prediction and validating solar radiation. *Journal of the Egyptian Mathematical Society* **27**, 47.

Mussa, Z. H., Othman, M. R. & Abdullah, M. P. 2015 Electrochemical oxidation of landfill leachate: investigation of operational parameters and kinetics using graphite-PVC composite electrode as anode. *Journal of the Brazilian Chemical Society* **26** (5), 939–948.

Nadeem, K., Guyer, G. T., Keskinler, B. & Dizge, N. 2019 Investigation of segregated wastewater streams reusability with membrane process for textile industry. *Journal of Cleaner Production* **228**, 1437–1445.

Neill, C. O., Hawkes, F., Hawkes, D., Lourenço, N., Pinheiro, H. & Delee, W. 1999 Colour in textile effluents–sources, measurement, discharge consents and simulation: a review. *Journal of Chemical Technology & Biotechnology* **74**, 1009–1018.

Panizza, M. & Cerisola, G. 2005 Application of diamond electrodes to electrochemical processes. *Electrochimica Acta* **51**, 191–199.

Periyasamy, S. & Muthuchamy, M. 2018 Electrochemical oxidation of paracetamol in water by graphite anode: effect of pH, electrolyte concentration and current density. *Journal of Environmental Chemical Engineering* **6**, 7358–7367.

Radjenovic, J. & Sedlak, D. 2015 Challenges and opportunities for electrochemical processes as next-generation technologies for the treatment of contaminated water. *Environmental Science & Technology* **49** (19), 11292–11302.

Rajkumar, K. & Muthukumar, M. 2017 Response surface optimization of electro-oxidation process for the treatment of C.I. Reactive Yellow 186 dye: reaction pathways. *Applied Water Science* **7**, 637–652.

Rice, E., Baird, R. & Eaton, A. 2017 *Standard Methods for the Examination of Water and Wastewater*. American Public Health Association, American Water Works Association, Water Environment Federation, USA.

Saleh, M., Yalvaç, M., Arslan, H. & Gün, M. 2019a Malachite Green dye removal from aqueous solutions using invader *Centaurea solstitialis* plant and optimization by response surface method: kinetic, isotherm, and thermodynamic study. *European Journal of Science and Technology* **17**, 755–768.

Saleh, M., Yalvaç, M. & Arslan, H. 2019b Optimization of remazol brilliant blue R adsorption onto *Xanthium italicum* using the response surface method. *Karbala International Journal of Modern Science* **8** (1(8)), 54–63.

Särkkä, H., Bhatnagar, A. & Sillanpää, M. 2015 Recent developments of electro-oxidation in water treatment – A review. *Journal of Electroanalytical Chemistry* **754**, 46–56.

Sirés, I., Brillas, E., Oturan, M., Rodrigo, M. & Panizza, M. 2014 Electrochemical advanced oxidation processes: today and tomorrow. A review. *Environmental Science and Pollution Research International* **21** (14), 8336–8367.

Soares, P., Souza, R., Soler, J., Silva, T., Guelli, S., Boaventura, R. & Vilar, V. 2017 Remediation of a synthetic textile wastewater from polyester-cotton dyeing combining biological and photochemical oxidation processes. *Separation and Purification Technology* **172**, 450–462.

Taherkhani, S., Darvishmotavalli, M., Bina, B., Karimyan, K., Fallahi, A. & Karimi, H. 2018 Dataset on photodegradation of tetracycline antibiotic with zinc stannate nanoflower in aqueous solution-application of response surface methodology. *Data Brief* **19**, 1997–2003.

Tavares, M., da Silva, L., Sales Solano, A., Tonholo, J., Martinez-Huitle, C. & Zanta, C. 2012 Electrochemical oxidation of methyl red using Ti/Ru0.3Ti0.7O$_2$ and Ti/Pt anodes. *Chemical Engineering Journal* **204–206**, 141–150.

Ukundimana, Z., Omwene, P., Gengec, E., Can, O. & Kobya, M. 2018 Electrooxidation as post treatment of ultrafiltration effluent in a landfill leachate MBR treatment plant: effects of BDD, Pt and DSA anode types. *Electrochimica Acta* **286**, 252–263.

Verma, A., Dash, R. & Bhunia, P. 2012 A review on chemical coagulation/flocculation technologies for removal of color from textile wastewaters. *Journal of Environmental Management* **93** (1), 154–168.

Yabalak, E. & Yilmaz, Ö. 2019 Eco-friendly approach to mineralise 2-nitroaniline using subcritical water oxidation method: use of ANN and RSM in the optimisation and modeling of the process. *Journal of the Iranian Chemical Society* **16**, 117–126.

Yagub, M., Sen, T., Afroze, S. & Ang, H. 2014 Dye and its removal from aqueous solution by adsorption: a review. *Advances in Colloid and Interface Science* **209**, 172–184.

Yalvaç, M., Arslan, H., Saleh, M., Gün, M. & Hekim, M. Ş. 2020 Utilizing of bio-adsorbent in zero waste concept: adsorption study of crystal violet onto the *Centaurea solstitialis* and *Verbascum thapsus* plants. *Pamukkale University Journal of Engineering Sciences* **27**, 349–358.

Zhang, O., Lin, B., Chen, Y., Gao, B., Fu, L. & Li, B. 2012 Electrochemical and photoelectrochemical characteristics of tinbo5 nanosheet electrode. *Electrochimica Acta* **81**, 74–82.

Zhu, C., Jiang, C., Chen, S., Mei, R., Wang, X., Cao, J., Ma, L., Zhou, B., Wei, Q., Ouyang, G., Yu, Z. & Zhou, K. 2018 Ultrasound enhanced electrochemical oxidation of Alizarin Red S on boron doped diamond(BDD) anode:effect of degradation process parameters. *Chemosphere* **209**, 685–695.